ELSEVIER

Earth and Planetary Science Letters 152 (1997) 251–265

EPSL

The origin of abyssal peridotites: a new perspective

Yaoling Niu [a,*], Charles H. Langmuir [b], Rosamond J. Kinzler [b]

[a] *Department of Earth Sciences, The University of Queensland, Brisbane, Qld 4072, Australia*
[b] *Lamont–Doherty Earth Observatory, Palisades, NY 10964, USA*

Received 15 October 1996; revised 7 July 1997; accepted 7 July 1997

Abstract

Abyssal peridotites have been interpreted to be residues of mantle melting beneath ocean ridges. Recent experimental data and models of mantle melting allow quantitative tests of this hypothesis. The tests show that abyssal peridotites are not purely melting residues. Their modal proportions and whole-rock compositions have far more olivine than would be predicted from melting models. Nonetheless, the correlations between modal proportions of olivine and residual mineral chemistry, and the relationship between associated basalt and peridotite compositions, require an important role for melting. We suggest that abyssal peridotite compositions result from a combination of melting and crystallization processes that are both a natural response to ascent of solid and melt beneath an ocean ridge. Different extents of melting create a range of residual peridotite and mantle melt compositions. The buoyant melts migrate upwards, where they encounter the surface thermal boundary layer and crystallize olivine. The greater the ambient extent of melting of the mantle, the higher the normative olivine contents of the melt, and the more melt is produced. Hence greater extents of melting lead to more olivine crystallization at shallow levels. This correlation between melting and crystallization within the mantle preserves the observed relationships between peridotite modes and mineral compositions. Significant implications of these results are: (1) the bulk composition of the oceanic crust differs from the primary melt compositions produced by partial melting of the mantle because of olivine crystallization at the thermal boundary layer; (2) the actual thickness of igneous crust may be variably thinner than would be calculated assuming total melt extraction; and (3) peridotite modes can be used to infer polybaric mantle melting reactions only if the accumulated olivine is removed appropriately. © 1997 Elsevier Science B.V.

Keywords: peridotites; mid-ocean ridge basalts; mantle; partial melting; mid-ocean ridges

1. Introduction

Abyssal peridotites and mid-ocean ridge basalts (MORB) are complementary products of the mantle melting and melt extraction processes that create the ocean crust. As such, they provide independent information on these processes, and conclusions coming from studies of the two materials can be tested for consistency. In recent years, there has been convincing agreement between results from abyssal peridotites and MORB. Studies of abyssal peridotites [1–3] have been used to infer different extents of melting of the mantle, in agreement with studies of MORB that led to the recognition of global correlations of chemical compositions with ridge depth [1–4] and crustal thickness [4], and that different extents of melting exert a primary control on MORB

* Corresponding author. Tel.: +61 7 3365 2372. Fax: +61 7 3365 1277. E-mail: niu@earthsciences.uq.edu.au

PII S0012-821X(97)00119-2

parental compositions. Indeed, Dick et al. [2] showed that variation in abyssal peridotites and spatially associated MORB are complementary in terms of the extent of mantle melting and proximity to mantle hotspots, and that the variations correlated with the geoid as well. Fig. 1 presents an updated view of this relationship, and shows that the amount of modal clinopyroxene in abyssal peridotites correlates with the Na_8 of spatially associated MORB. Varying extents of melting account qualitatively for the relationship between abyssal peridotites and MORB.

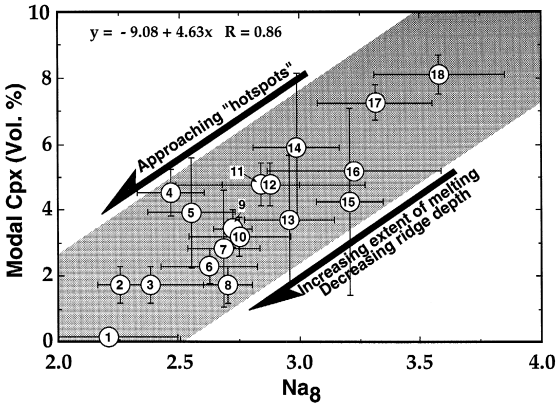

Fig. 1. Clinopyroxene modes in abyssal peridotites plotted against Na_8 of spatially associated MORB. Na_8 is the weight percent Na_2O in basalts corrected to a MgO value of 8 wt% to remove the effect of low-pressure fractionation, following [4]. This diagram is very similar to fig. 7 of [2], but we used Na_8 instead of normative plagioclase/clinopyroxene ratio used by these authors. Clinopyroxene modal data are from [2]. MORB data are from [11], and the compilations of [4,8]. The error bars for both clinopyroxene and Na_8 are 2σ of the averages for a given suite. The significant positive correlation reflects a compositional complementarity between abyssal peridotites and MORB; that is, the extent of melting inferred from MORB (decreasing Na_8) is accompanied by increasing depletion of a melt component in abyssal peridotites (decreasing clinopyroxene modes), and has been interpreted as resulting from variable amounts of melting due primarily to mantle temperature variation [2,4]. Ridges affected thermally by hotspots are characterized by higher extents of melting, thicker crust, and hence, shallower axial depth than normal ridges away from hotspots. *1* = near Azores (MAR); *2* = Bouvet FZ (far to Bouvet Island; SWIR); *3* = Islas Orcadas FZ (SWIR); *4* = Argo FZ (CIR); *5* = Marie Celeste FZ (CIR); *6* = Bouvet FZ (SWIR); *7* = Kane FZ (MAR); *8* = Axis—3°32′E (near Bouvet Island, SWIR); *9* = 54°S Rift (SWIR); *10* = 22°S FZ (MAR); *11* = Northeast Bullard (AAR); *12* = Bullard FZ (AAR); *13* = Atlantis II FZ, W. Wall (SWIR); *14* = Atlantis II FZ, E. Wall (SWIR); *15* = Cayman Trough (MCR); *16* = Northwest Bullard (AAR); *17* = Vulcan FZ (SWIR); and 18–26°S Rift (SWIR).

Although this first order relationship is robust, the quantitative melting models that have been applied to MORB have not yet been applied to abyssal peridotites. There have been indications that the results will not be straightforward. For example, Elthon [5] suggested that the bulk chemical compositions of abyssal peridotites are not consistent with their being straightforward residues of batch or fractional melting. He proposed instead that the chemical trends of abyssal peridotites result predominantly from refertilization processes rather than from partial melting processes. Clearly, in order to fully understand the nature of melting and crustal accretion processes beneath mid-ocean ridges, the constraints from MORB and abyssal peridotites need to be reconciled quantitatively. In this paper we take a first step in that direction by showing the importance of olivine accumulation to abyssal peridotite modes and bulk chemical compositions.

There are many second order aspects of melt generation and crustal accretion which can be addressed independently through studies of abyssal peridotites and MORB, and which ultimately need to be reconciled. These second order aspects, which may be collectively termed mantle melting dynamics, include the initial and final depths of melting, the melting rate, the extent to which melting is fractional or batch, extent and depth of melt–rock interaction, modal and chemical source variation, etc. The nature of these processes has been addressed to varying extents using both MORB and abyssal peridotite data, and are still subject to debate [4,6–16]. In this paper we compare major element systematics and mineral modes preserved in the bulk-rock abyssal peridotites with mantle melting models and assess the role of major element source variation in the generation of the observed major element variability of abyssal peridotites. A more comprehensive treatment, which considers the details of polybaric melting and our diverse views of the implications of these results will be presented elsewhere (Niu [17]; Kinzler and Langmuir, in prep.).

2. Evidence from abyssal peridotites modes

The most robust observations pertinent to the study of abyssal peridotites are volume percent

modes, as originally described by Dick et al. [2]. An updated compilation of abyssal peridotite modes is presented in Fig. 2. The modes show progressively decreasing amounts of clinopyroxene and increasing olivine, which qualitatively appears to be consistent with a progressive melting trend, as emphasized by Dick and co-authors [1,2,6,11] and Michael and Bonatti [3]. As it is generally agreed that the mean pressure of MORB generation is on the order of 8–20 kbar [7–10], a quantitative test can be conducted by comparing abyssal peridotite modal systematics with melting paths constrained by the experimental data [9,18–20]. Fig. 2 compares the abyssal peridotite modal data with the peridotite melting paths from a mineralogically similar source at 10 and 20 kbar. It is clear that modal systematics of abyssal peridotites are not consistent with isobaric melting residues at pressures greater than 10 kbar nor with polybaric near-fractional melting residues calculated over this pressure range [17]. Thus abyssal peridotites are not derived purely by progressive melting of compositionally similar sources.

The abyssal peridotite modal systematics in Fig. 2 could be the combined result of progressive melting and fertile mantle mineralogical variation. Indeed, fertile mantle heterogeneity is well known to exist on various scales such as modal heterogeneity in mantle xenoliths and lithological variations such as clinopyroxenite layers/veins in peridotite massifs [21]. If this were the case, the fertile mantle mineralogy would have to vary substantially in its ratio of orthopyroxene to olivine. Melting such sources with variable orthopyroxene/olivine ratios between 10 and 20 kbar would explain the large modal variability of abyssal peridotites. The problem with this explanation lies in generating such a source variation. Melting reactions create vertical variation in this diagram, while the source variation required to explain the peridotite data is more or less horizontal. Mantle melting processes at moderate pressures do not generally create large variations in the orthopyroxene/olivine ratio. Furthermore, the abyssal peridotite modes show a clearly defined trend in Fig. 2, with the pyroxene-poor and olivine-rich end being associated with mantle hotspots/plumes (e.g., the Bouvet hotspot) whose fertile source peridotites should be enriched, not depleted, in clinopyroxene. Therefore, the trend of the abyssal peridotite data is not consistent with mantle melting at pressures appropriate for the oceanic crust formation, nor can the trend be explained readily by fertile mantle mineralogical variation.

An alternative explanation would be to create the abyssal peridotite trend by adding olivine to residues

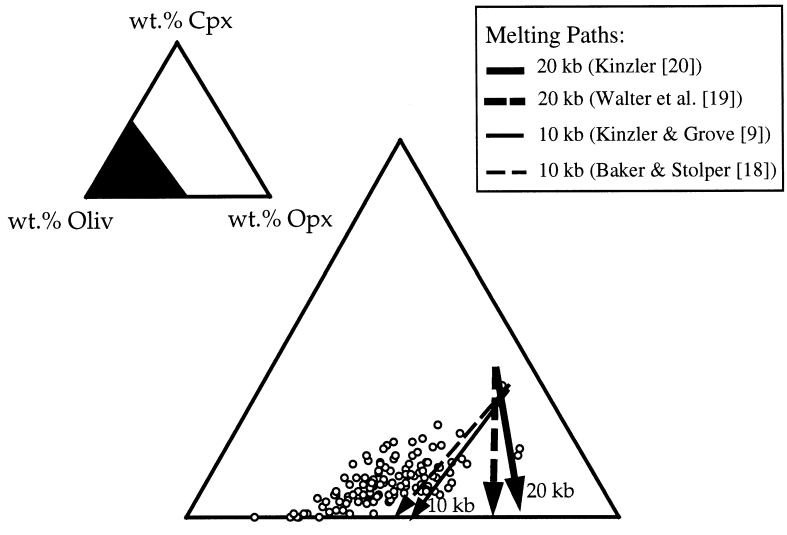

Fig. 2. Weight percent modes (converted from volume percent using [48,49]) for the abyssal peridotite data set compiled for this study [1,2,6,11,33]. Isobaric melting paths determined experimentally at 10 and 20 kbar are shown.

produced by progressive amounts of melting. Olivine addition would create the linear trend of the data, and explain the large range in orthopyroxene/olivine ratio that is observed. In the next section we develop methods to examine the bulk compositions of abyssal peridotites, as any model for the origin of abyssal peridotite must be consistent with both modal and bulk chemical data.

3. Evidence from reconstituted whole-rock compositions

Bulk compositions are the primary tool of igneous petrologists for the understanding of petrogenesis. However, the compositions of abyssal peridotites relevant to melting and melt transport are not straightforward to determine. Abyssal peridotites are metamorphic rocks with complex histories of deformation [15,22–25], and evidence of veining and melt impregnation [2,24–28]. Most abyssal peridotites also have experienced sub-solidus re-equilibration at pressures and temperatures well below those of mantle melting [29,30] and are serpentinized and weathered to various extents [1,24–31]. For these reasons, and because of their large grain sizes relative to recovered hand specimens, direct whole-rock analyses of abyssal peridotites do not reflect the chemical compositions pertinent to studies of mantle melting. In order to overcome these various problems, we have reconstructed bulk-rock compositions based on reported mineral proportions and electron microprobe analyses [2,5,32]. These reconstructed compositions should reflect more faithfully the igneous record in these rocks.

3.1. Data treatment

A substantial amount of abyssal peridotite data exists in the literature [1–3,6,24–31,33–47]. In this study we have used only peridotites for which modal analyses and mineral analyses are available. This reduces our data set to those discussed by Dick and Fisher [1], Dick et al. [2], Dick [33], Johnson et al. [6], and Johnson and Dick [11]. To avoid the chemical effects of melt impregnation, we have selected only those abyssal peridotites with $< 2\%$ plagioclase, which itself is excluded in the calculation. Our data set thus consists of spinel-bearing lherzolites and harzburgites. Note that samples from intermediate and fast spreading ridges do not occur in the published abyssal peridotite database.

To construct the whole-rock compositions, we converted the mineral modes to weight fractions (f_j) using calculated mineral densities at $P = 1$ bar and $T = 25°C$ [48,49]. The whole-rock composition for each oxide (Ox_i) in each sample is calculated from:

$$Ox_i^{wr} = \sum_{j=1}^{n} f_j Ox_i^j \quad (1)$$

where the subscript i refers to oxides (SiO_2, TiO_2, Al_2O_3, Cr_2O_3, FeO, MnO, MgO, CaO, Na_2O), and j refers to mineral phases (olivine [ol], orthopyroxene [opx], clinopyroxene [cpx], and spinel [sp]).

In the entire data set of 132 samples for which modes have been published, only 33 samples have analyses of all four phases (ol, opx, cpx, and sp). Other samples often have only two or three phases analyzed, which prevents direct calculation of whole-rock compositions for the entire data set. However, mineral compositions are highly correlated in the data set, which permits a robust estimate of the compositions of unanalyzed phases (see the appendix in the **EPSL Online Background Dataset** [1]).

3.1.1. Potential errors in reconstituted whole-rock compositions

As discussed above and detailed in the appendix (in the **EPSL Online Background Dataset** [2]), the procedure for calculating the whole-rock composition involves predicting the composition of an unanalyzed mineral from the compositions of coexisting phases, which may introduce uncertainties into the estimate of the bulk rock compositions. Because the variability in modes greatly exceeds that of the compositions of the minerals, the uncertainties in mineral compositions do not contribute significantly. Table 1 compares the percent standard deviations of mineral

[1] http://www.elsevier.nl/locate/epsl, mirror site: http://www.elsevier.com/locate epsl.

[2] http://www.elsevier.nl/locate/epsl, mirror site: http://www.elsevier.com/locate epsl.

Table 1
Mean and relative variability of mineral modes and mineral compositions (SiO_2, FeO, MgO and $Mg^{\#}$) of abyssal peridotites

	Mode (vol.%)	SiO_2 (wt%)	FeOt (wt%)	MgO (wt%)	$Mg^{\#}$
Olivine					
Mean	73.64	40.54	9.45	49.25	90.29
1σ	6.25	0.29	0.36	0.36	0.37
RSD%	8.48	0.71	3.78	0.73	0.41
RSD/RSD_{Mode}	1.00	0.08	0.45	0.09	0.05
Orthopyroxene					
Mean	20.68	54.31	5.91	32.25	90.68
1σ	4.41	0.68	0.36	0.93	0.55
RSD%	21.30	1.24	6.02	2.89	0.61
RSD/RSD_{Mode}	1.00	0.15	0.71	0.34	0.03
Clinopyroxene					
Mean	4.92	50.84	2.81	17.01	91.56
1σ	2.62	0.62	0.44	1.35	0.86
RSD%	53.32	1.22	15.57	7.93	0.94
RSD/RSD_{Mode}	1.00	0.02	0.29	0.15	0.02
Spinel					
Mean	0.68	–	13.73	18.36	
1σ	0.35	–	2.36	1.69	
RSD%	50.61	–	17.23	9.23	
RSD/RSD_{Mode}	1.00	–	0.34	0.18	

Total Fe as FeO. 1σ is one standard deviation. RSD% is the relative standard deviation in percent (i.e., $1\sigma/\text{Mean}\times 100$). Data are from [1,2,6,11,33].

compositions (SiO_2, FeO and MgO) and modes. The relative variation in modes is significantly greater than that of the mineral compositions. Since the reconstructed whole-rock compositions reflect the sum of the product of mode and composition, the whole-rock compositional variation is largely determined by modal mineralogy. The significant correlations of the calculated whole-rock oxides with mineral modes in Fig. 3 further demonstrate that the whole-rock composition of abyssal peridotites is controlled by mineral modes, particularly the abundance

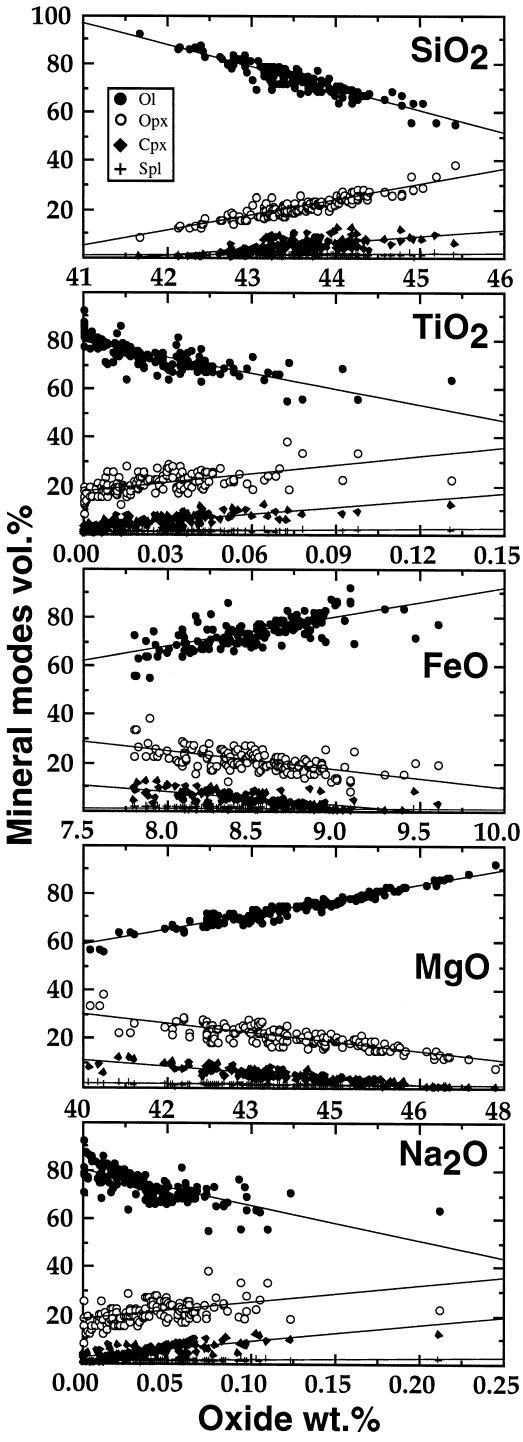

Fig. 3. Abyssal peridotite modes (vol.%) of olivine, orthopyroxene, clinopyroxene, and spinel plotted against the reconstructed whole-rock oxides (wt%) SiO_2, TiO_2, FeO, MgO, and Na_2O. The solid lines passing through the data are linear regression lines. Although the correlations of these whole-rock oxide abundances with mineral modes are expected, these correlations emphasize that the reconstructed whole-rock compositions are determined primarily by mineral modes.

of olivine (55–90%). Thus, the principal source of variation in the reconstituted bulk compositions of abyssal peridotites is the modal variation.

A potential error may stem from uncertainties in modal analysis. Most seriously, serpentinization of olivine can be associated with a 20–30% volume increase, and we must consider whether this could lead to a serious overestimation of the modal olivine. However, ol, opx and cpx are all subject to serpentinization, as pointed out in this context by Komor et al. [46], although serpentinization rates decrease in general in the order ol, opx, cpx [50]. Because olivine and orthopyroxene make up 90% or more of the rocks, a volume increase of these two phases has almost no effect on the relative proportions of the phases. For example, if a rock has 5% modal clinopyroxene, 75% olivine and 20% orthopyroxene, a 25% volume increase caused by serpentinization of the olivine and opx would lead to apparent modes of 4% cpx, 75.8% olivine and 20.2% opx. These changes contribute trivially to the noise of the data. Recently, Dick (pers. commun.) observed in Hess Deep peridotites [51] that there is a general tendency that more serpentinization occurs in more olivine-rich peridotites, implying that there would be a progressively greater overestimation of olivine modes in more olivine-rich rocks if volume expansion due to serpentinization is not properly corrected for. However, as the modal olivine difference before and after serpentinization correction is constant ($\leq 2\%$, after Dick, pers. commun.), and is independent of the amounts of olivine and serpentine in the rocks, the error contributes little to the calculated bulk-rock compositional systematics (e.g., about ~ 0.2 wt% random errors associated with bulk-rock FeO of all samples).

Since the procedure to estimate the composition of an unanalyzed phase is based on correlations that exist within the data set, the question arises whether this procedure may cause better correlations in the reconstructed data than exist in the raw data. This is certainly true for the specific plots of mineral composition shown in fig. A1 (see the **EPSL Online**

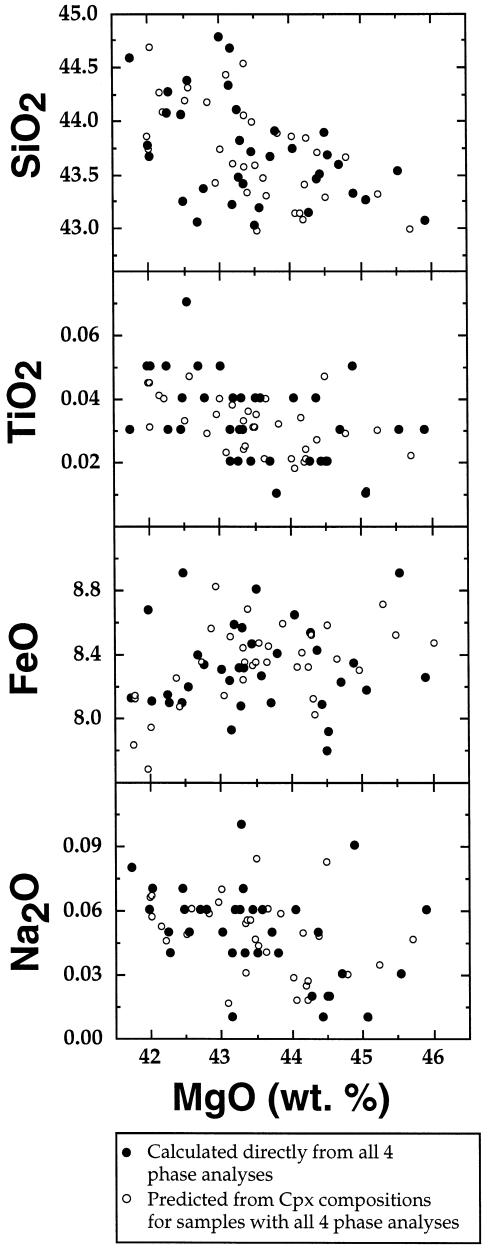

Fig. 4. Plots of SiO_2, TiO_2, FeO and Na_2O versus MgO to compare reconstructed whole rock compositions determined using calculated mineral compositions (see Appendix and Fig. A2 in the **EPSL Online Background Dataset** (http://www.elsevier.nl/locate/epsl, mirror site: http://www.elsevier.com/locate epsl)) with whole rock compositions reconstructed directly from actual mineral compositions. Note that the systematics of the data are quite similar. Therefore the procedure used to determine whole rock compositions when only a few of the mineral compositions have been determined is reliable.

Background Dataset [3]) — reconstructing these data from the regression lines would force the data onto a single line on each of these mineral composition plots. The question is whether it also leads to linearity among the reconstructed whole-rock compositions. This is not self-evident, since most of the variation in the whole-rock compositions comes from variations in modal abundances rather than mineral compositions, as discussed above. Any systematic errors associated with the reconstructed whole rocks can be estimated by reconstructing the subset of the abyssal peridotite data set for which the compositions of all 4 phases (ol, cpx, opx and sp) are reported. These calculated data can be compared with the actual data, to see if the calculation imposes additional systematics. This test is shown in Fig. 4 (see also fig. A2 in the **EPSL Online Background Dataset** [4]). There is no enhanced linearity in the reconstructed data, therefore the reconstructed data are reliable.

3.2. Comparison of melting models

From the above discussion we can see that we can approach the reconstituted whole-rock abyssal peridotite compositions with reasonable confidence. In order to understand the petrogenetic implications of the reconstituted bulk compositions we need to be able to compare them to those that would be predicted from various melting processes. This requires a modelling approach due to the potential complexity and diversity of the mantle melting process. The question then arises to what extent the results depend on the particular model used. Each of us has constructed a mantle melting model [7,10,20] and the three models stem from entirely different approaches. A comparison of the three models gives an indication of to what extent interpretations can be made that are model independent. Fig. 5 shows results for MgO versus FeO for the three different models, starting from the same source composition. The models cover a large range of variables (from polybaric, fractional melting starting at two different pressures to isobaric batch melting at two different pressures). It is clear that the models agree on the essential characteristics of the FeO–MgO variation: FeO changes little as melting proceeds at these pressures, and higher pressures of melting lead to slightly lower FeO contents in the residues. The general agreement among the models extends to the other oxides as well. Because of this overall agreement, for the sake of clarity in the figures, the following discussion occurs with reference to the Niu and Batiza [7] model. Either of the other two models also would have sufficed. Although there is general agreement for calculations of the residues, the agreement does not extend to the integrated melts. Calculation of integrated melts requires estimation of the mixing and melting functions [10] and requires assumptions on whether or not melt extraction is complete, and the three melting models differ in these aspects. These differences do not influence the discussion of abyssal peridotites presented here.

3.3. Comparison of melting models to abyssal peridotite whole-rock compositions

Reconstituted whole-rock abyssal peridotite compositions are presented in Fig. 6. Residual mantle

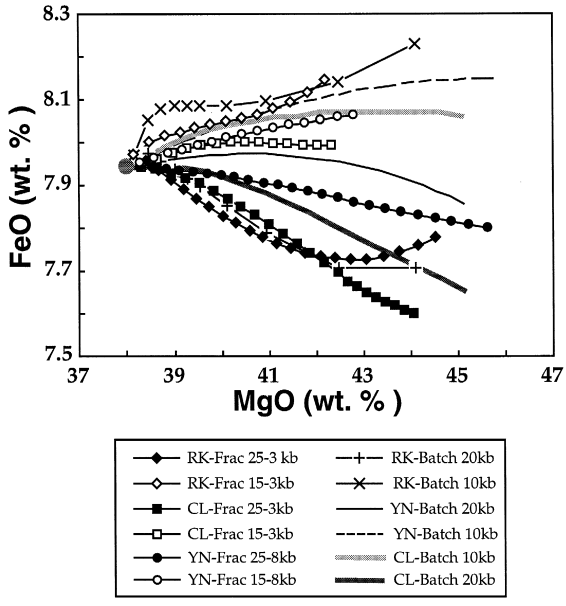

Fig. 5. Comparison of 3 melting models (FeO versus MgO), isobaric at 10 and 20 kbar and polybaric, starting at 25 and 15 kbar. The starting source composition (shaded circle) is listed in caption for Fig. 6.

[3] http://www.elsevier.nl/locate/epsl, mirror site: http://www.elsevier.com/locate epsl.

[4] http://www.elsevier.nl/locate/epsl, mirror site: http://www.elsevier.com/locate epsl.

compositions calculated for batch and near fractional melting are shown for comparison. The source composition used for the models is within the range of mantle compositions suggested in the literature (see caption for Fig. 7) with values chosen to be most consistent with the abyssal peridotite data, and recognizing that the MORB source must be depleted in incompatible elements relative to primitive mantle compositions. (Thus, whatever primitive mantle composition is chosen, the Na_2O and TiO_2 residing in the continental crust need to be removed.) The source composition used is reported in the caption for Fig. 6.

Elthon [5] and Langmuir et al. [10] first pointed out that the MgO–Na_2O systematics of peridotite whole-rock compositions are not consistent with melting models. Fig. 6 confirms this conclusion for Na_2O and shows that it applies to TiO_2, SiO_2 and FeO as well (CaO and Al_2O_3 are not shown because melt extraction and olivine addition are not distinguishable on these diagrams). The batch melting curves for TiO_2 and Na_2O plot closer to the data; however, the highest density of data still plots above these curves. The slopes of the SiO_2 and FeO data are clearly inconsistent with either melting model. We emphasize that this conclusion applies to all three calculated melting models.

The steepness of the positive MgO–FeO correlation, in particular, contrasts with the melting curves. This conclusion differs from that of Elthon [5], who observed a more shallow FeO–MgO slope. We attribute the difference between our data and Elthon's

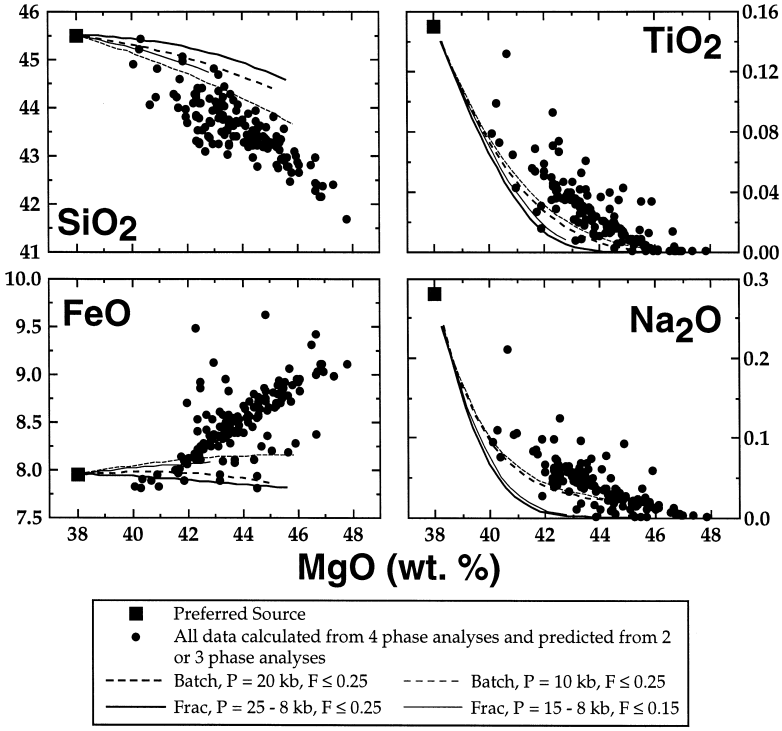

Fig. 6. MgO variation diagrams of representative oxides (SiO_2, TiO_2, FeO, and Na_2O) of the reconstructed bulk abyssal peridotite compositions. Model melting residues produced by polybaric near-fractional (1% melt porosity) melting with initial melting depths of P_o = 15 (F = 1–15%) and 25 (F = 1–25%) kbar, and by isobaric batch melting at P = 10 and 20 (F = 1–25% for both) kbar are also plotted for comparison. The model residues are calculated using the method of [7,17] modified by incorporating more recent peridotite experimental data of [18,62]. The starting composition used is (wt%): SiO_2 = 45.5; TiO_2 = 0.15; Al_2O_3 = 4.17; Cr_2O_3 = 0.36; FeO = 7.94; MnO = 0.10; MgO = 38.0; CaO = 3.11; Na_2O = 0.28; K_2O = 0.007. Note that at a given MgO value, Na_2O and TiO_2 abundances are higher than in calculated residues, but closer to those of batch melting than fractional melting. Importantly, SiO_2 is significantly lower, and FeO is significantly higher than expected for residues produced by either model. The positive MgO–FeO correlation is totally unexpected, indicating that abyssal peridotites are not purely melting residues.

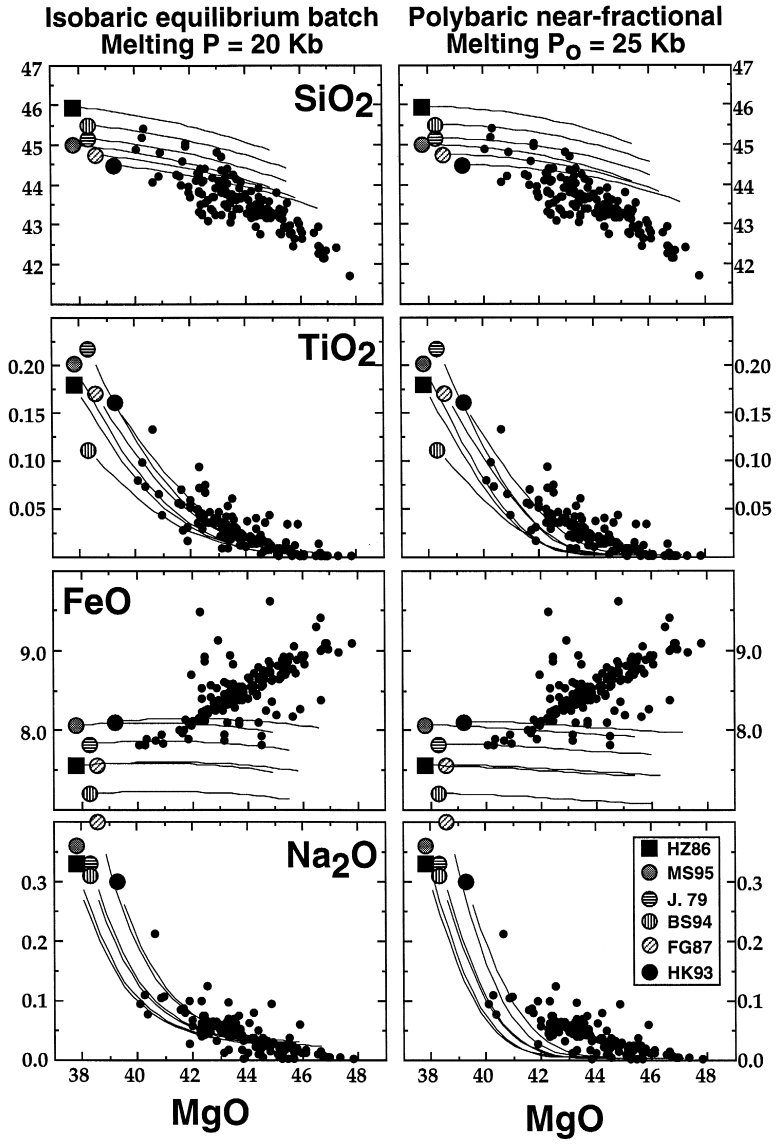

Fig. 7. MgO variation diagrams of SiO_2, TiO_2, FeO, and Na_2O to show that the chemical systematics of abyssal peridotites are not caused by mantle source compositional variation. The lines are model residues produced by isobaric 'batch' melting (left) and polybaric near-fractional (1% melt retention) melting (right) as described in Fig. 6. Different symbols represent several possible fertile mantle compositions for MORB. HZ86 is the primitive upper mantle of [63]. MS95 is the primitive mantle (or bulk silicate earth) of [64]. J. 79 is the model mantle composition of [65]. BS94 is the model composition MM3 of [18]. FG87 is the MORB pyrolite 90 of [57]. HK93 is KLB-1, a less fertile peridotite, thought to be more appropriate for MORB mantle, used in melting experiments by [62]. Whereas the actual compositional variation of MORB mantle is unknown, its variation ranges in terms of SiO_2, TiO_2, FeO, MgO, and Na_2O are unlikely to be larger than the ranges of these peridotites. Several important points are: (1) although the fertile source compositions may be expected to vary for abyssal peridotites, the SiO_2–MgO and FeO–MgO relationships defined by abyssal peridotites cannot be explained by source compositional variation, as the melting trends intersect the abyssal peridotite trends at a high angle; (2) at a given MgO, the variation ranges of Na_2O and TiO_2 for the majority of the abyssal peridotite data may be explained qualitatively by source compositional variation; and (3) regardless of the source compositional variation, curves for 'batch' melting plot closer than near-fractional melting to the data for TiO_2–MgO and Na_2O–MgO.

on this diagram to the restricted range of MgO content of the peridotites that Elthon was able to consider. The reconstitution calculations described above allow the consideration of a much larger data set, and therefore lead to a more robust characterization of the compositional variation present in the abyssal peridotite data set. The lack of agreement between the abyssal peridotite data and the melting models requires that some processes other than polybaric melting must contribute to the systematics of the data. In the following sections we consider possible explanations.

3.3.1. Source variations

To evaluate the potential effects of mantle source compositional variation on melting residues, we have plotted 6 mantle sources, and the model residues produced by partial melting of these sources in Fig. 7. The polybaric, near-fractional melting curves fail to account for the trends of the data for any of the four oxides. Although the isobaric, batch melting curves for TiO_2 and Na_2O do appear to pass through the data fields, isobaric, batch melting curves do not pass through the data for SiO_2 and FeO, nor do they have slopes that resemble the slopes of the melting curves. The slopes of the abyssal peridotite whole-rock data on the SiO_2–MgO and FeO–MgO plots are much steeper than those of model residues regardless of source compositions and models used. Since a successful model must simultaneously account for all the oxides, it is clear that source heterogeneity, combined with either fractional or batch melting, does not successfully explain the compositional variations observed in the reconstituted abyssal peridotite data (also noted by Elthon [5] in terms of MgO–Na_2O systematics).

3.3.2. The effects of olivine addition

As previous workers have noted, peridotites in general, and abyssal peridotites in particular, define near-linear trends on variation diagrams, which is suggestive of an origin through mixing [5,10]. The depleted mixing end-member has high MgO, high FeO, low SiO_2, and no CaO, Al_2O_3, TiO_2, and Na_2O. An obvious candidate for such an end-member is olivine. Indeed, as shown in Figs. 2 and 3,

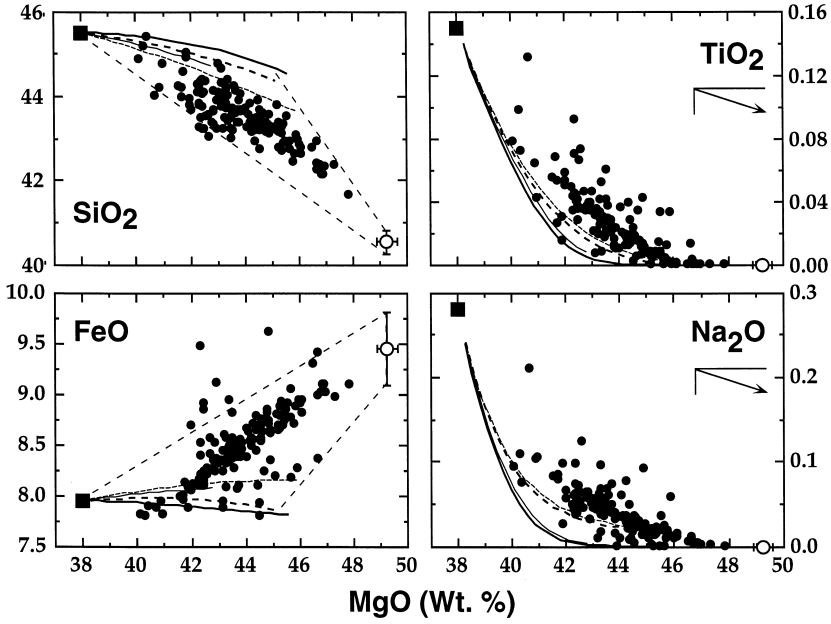

Fig. 8. MgO variation diagrams for SiO_2, TiO_2, FeO, and Na_2O with abyssal peridotite data, and model residues as in Fig. 6. Also plotted is the mean composition of olivine in abyssal peridotites with error bars (2σ). Clearly, the trends defined by the majority of the abyssal peridotite data on the SiO_2–MgO and FeO–MgO plots are consistent with accumulation of olivine. The fields enclosed by the dashed lines are where the mixtures may be expected assuming the residues are produced by variable amounts of melting from compositionally similar sources.

many abyssal peridotites have very high (> 80%) modal olivine, significantly in excess of what would be predicted for residues of mantle melting. Fig. 8 shows the mean composition of abyssal peridotite olivine on MgO variation diagrams. Mixing lines between such an olivine and the model melting curves account well for the abyssal peridotite data. Olivine addition increases FeO and MgO and decreases SiO_2 in the whole rock. The dashed lines enclose fields that would result from mixing of olivine with diverse residues produced by melting a uniform source. The hint of curvature on the TiO_2–MgO and Na_2O–MgO plots suggest that some contribution from a primary melting signature may be preserved. Note that the steep FeO–MgO trend cannot be interpreted as opx removal as would be expected by melt–rock reaction associated with replacive dunites in mantle sections of mantle ophiolites [15,16,22,52]. This is because, although pyroxenes would also plot on the same 'addition/subtraction' line defined by the whole-rock data and olivine in FeO–MgO space, because they all have essentially the same FeO/MgO ratios, both opx and cpx have different FeO/SiO_2 and MgO/SiO_2 ratios than olivine, and thus they do not plot on the same 'addition/subtraction' line in FeO–SiO_2 and SiO_2–MgO spaces. Therefore, the abyssal peridotite data are inconsistent with melt–rock reaction but consistent with olivine crystallization, which has been quantitatively evaluated [17].

If olivine addition were a random process, it could effectively decouple the mineral mode from the mineral compositions. One of the primary observations for abyssal peridotites, however, is that modal proportions correlate with residual mineral chemistry [2,6]. This relationship is preserved because the amount of olivine added changes systematically with the extent of depletion of the residue — and hence the extent of partial melting. This can be illustrated by the mixing lines shown in Fig. 8 between average abyssal peridotite olivine and the calculated polybaric near fractional melting residues. In general, more depleted residues (higher MgO of residue) have accumulated greater amounts of excess olivine. This regularity is what preserves changes in abyssal peridotite mineral modes that are broadly consistent with melt extraction despite the fact that abyssal peridotites are not purely melting residues.

4. A petrogenetic model

We have demonstrated the importance of olivine addition as a fundamental control on abyssal peridotite modes and chemical compositions. Olivine addition alone, however, is not sufficient. For abyssal peridotites, variable extents of melting are required to provide the diversity of mixing end-members and to account for the changes in mineral composition. For MORB, variable extents of melting are required to account for the diversity of volcanic compositions. In addition, there is the relationship between abyssal peridotites and MORB documented by Dick et al. [2], where those regions for which MORB are derived by the greatest extent of melting have the most depleted abyssal peridotite residues. Therefore a

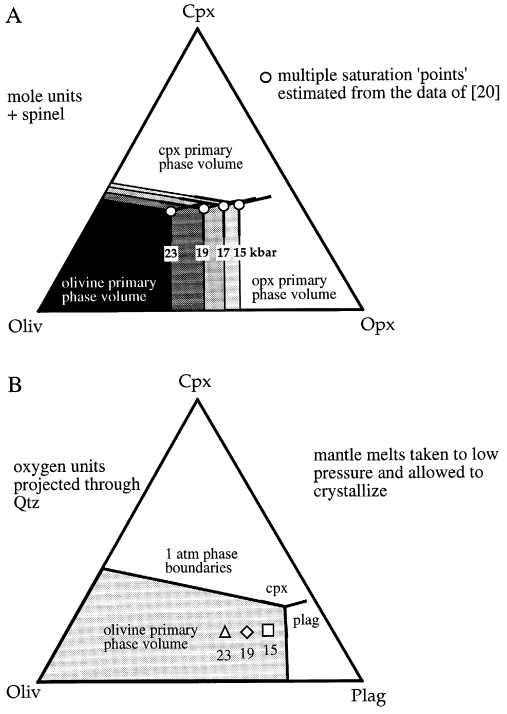

Fig. 9. (a) A schematic cartoon of the lower portion of a cpx–ol–opx ternary 'phase' diagram showing that the stability fields of the three phases change with pressure. This qualitative diagram is constructed based on the data of [20]. Multiple saturation boundaries at different pressures are projected as points for simplicity. These boundaries move away from olivine apex with decreasing pressure. (b) A schematic diagram showing the result of placing mantle melts generated at greater pressures at low pressures and allowing them to crystallize. The melts all lie in the olivine primary phase volume, and thus olivine will be the liquidus phase.

model which includes a variable extent of melting and variable amounts of olivine addition is necessary. The model must also account for the observation that the more depleted residues have accumulated greater amounts of olivine.

A useful starting point in constructing a model is the recognition that abyssal peridotites are likely to be samples from the top of the melting region and, furthermore, that the narrow zone of crustal accretion at mid-ocean ridges requires that melts generated over a wide region and depth range in the upper mantle be focused through a narrow zone beneath the ridge. Since this zone of melt focusing is likely to be shallow, near the surface, and within the thermal boundary layer, magmas passing through it will cool and crystallize whatever mineral is on their liquidus. One of the best established facts of experimental petrology is the expansion of the olivine primary phase volume with decreasing pressure [53–59] (Fig. 9a). This expansion will cause olivine to be the liquidus phase at shallow pressures (Fig. 9b). Therefore the combination of the physical setting with the phase equilibria leads to olivine crystallization as an inevitable consequence of the ascent and cooling of mantle melts.

That more olivine has been added to the most depleted abyssal peridotites is also a natural consequence of the melt generation process. Mantle melts vary in their normative olivine content, depending on the pressure [59] and extent of melting by which they were derived. Where melting begins deeper, the mantle melts to a greater extent, leading to residues that are more depleted, a larger melt volume, and melt compositions that are richer in normative olivine. Consequently, the most depleted residues are inevitably coupled with olivine-rich melts. These melts have more capacity to crystallize olivine as they cool during ascent.

The petrogenesis of abyssal peridotites thus appears as a natural consequence of the melting and cooling processes that take place beneath ocean ridges (Fig. 10). Variable extents of melting lead to a range of mantle residues, and olivine crystallization during ascent leads to olivine addition, with the amount correlating with the residue depletion. Since the thermal boundary layer at the earth's surface inevitably results in cooling during ascent, crystallization of olivine is a natural consequence of the melt generation and transport processes that create the oceanic crust.

5. Summary

There are several broad petrogenetic implications of the results discussed above:

1. Abyssal peridotites are not simple residues of mantle melting beneath ocean ridges, but are modified by the addition of olivine resulting from cooling and crystallization of ascending melts in the thermal boundary layer.
2. The thermal boundary layer extends below the Moho into the mantle. The thickness of this boundary is not well constrained at present but is likely to increase with decreasing spreading rate [60], which has been reiterated recently with evidence [61].

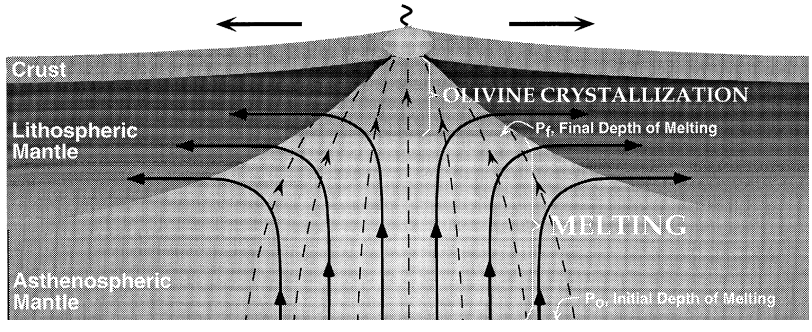

Fig. 10. A cartoon to account for the olivine-rich modes of abyssal peridotites. Melting stops at a final pressure of melting (P_f) some depth beneath the crust in the mantle. Cooling of melt in this region leads to olivine accumulation in the previously depleted melting residues. The actual value of P_f is not constrained in the current paper, and the depth in the figure is schematic only. The thick lines with arrows are mantle flow lines; the dashed lines with arrows are schematic paths of melt migration towards the ridge axis.

3. The bulk composition of the oceanic crust is depleted in olivine relative to melts produced by mantle melting.
4. As the result of olivine subtraction from the primary melts produced by mantle melting, the thickness of the igneous ocean crust may be variably thinner than calculated assuming total melt extraction.

Acknowledgements

This work was supported by The University of Queensland, an LDEO postdoctoral Fellowship and Australian ARC grants to YN, and US NSF grants to CL and RK. YN also acknowledges the support from the Department of Industry, Science and Tourism of Australia (DIST, 94/7934), and the hospitality of IFREMER. Discussions with Roger Hékinian, Daniel Bideau, Joe Boyd, Peter Keleman, and Henry Dick were helpful. Thorough and critical reviews by Francis Albarède and Henry Dick are acknowledged with great gratitude. This is LDEO contribution 5681. ***[RV]***

References

[1] H.J.B. Dick, R.L. Fisher, Mineralogic studies of the residues of mantle melting: abyssal and alpine-type peridotites, in: J. Kornprobst (Ed.), Proc. the 3rd Int. Kimberlite Conference, Elsevier, Amsterdam, 1984, pp. 295–308.

[2] H.J.B. Dick, R.L. Fisher, W.B. Bryan, Mineralogical variability of the uppermost mantle along mid-ocean ridges, Earth Planet. Sci. Lett. 69 (1984) 88–106.

[3] P.J. Michael, E. Bonatti, Peridotite composition from the North Atlantic: Regional and tectonic variations and implications for partial melting, Earth Planet. Sci. Lett. 73 (1985) 91–l04.

[4] E.M. Klein, C.H. Langmuir, Global correlations of ocean ridge basalt chemistry with axial depth and crustal thickness, J. Geophys. Res. 92 (1987) 8089–8115.

[5] D. Elthon, Chemical trends in abyssal peridotites: Refertilization of depleted oceanic mantle, J. Geophys. Res. 97 (1992) 9015–9025.

[6] K.T.M. Johnson, H.J.B. Dick, N. Shimizu, Melting in the oceanic upper mantle: an ion microprobe study of diopside in abyssal peridotites, J. Geophys. Res. 95 (1990) 2661–2678.

[7] Y. Niu, R. Batiza, An empirical method for calculating melt compositions produced beneath mid-ocean ridges: application for axis and off-axis (seamounts) melting, J. Geophys. Res. 96 (1991) 21753–21777.

[8] Y. Niu, R. Batiza, Chemical variation trends at fast and slow spreading ridges, J. Geophys. Res. 98 (1993) 7887–7902.

[9] R.J. Kinzler, T.L. Grove, Primary magmas of mid-ocean ridge basalts, 2. Applications, J. Geophys. Res. 97 (1992) 6907–6926.

[10] C.H. Langmuir, E.M. Klein, T. Plank, Petrological systematics of mid-ocean ridge basalts: Constraints on melt generation beneath ocean ridges, in: J. Phipps Morgan, D.K. Blackman, J.M. Sinton (Eds.), Mantle Flow and Melt Generation at Mid-Ocean Ridges, AGU Geophys. Monogr. 71 (1992) 183–280.

[11] K.T.M. Johnson, H.J.B. Dick, Open system melting and the temporal and spatial variation of peridotite and basalt compositions at the Atlantis II F.Z., J. Geophys. Res. 97 (1992) 9219–9241.

[12] J.H. Natland, Partial melting of a lithologically heterogeneous mantle: Inferences from crystallisation histories of magnesian abyssal tholeiites from the Siqueiros Fracture Zone, in: A.D. Saunders, M.J. Norry (Eds.), Magmatism in Ocean Basins, Geol. Soc. London Spec. Publ. 42 (1989) 41–70.

[13] F. Albarède, How deep do common basaltic magmas form and differentiate?, J. Geophys. Res. 97 (1992) 10997–11009.

[14] Y. Shen, D.W. Forsyth, Geochemical constraints on initial and final depth of melting beneath mid-ocean ridges, J. Geophys. Res. 100 (1995) 2211–2237.

[15] P.B. Kelemen, H.J.B. Dick, Focused melt flow and localized deformation in the upper mantle; juxtaposition of replacive dunite and ductile shear zones in the Josephine Peridotite, SW Oregon, J. Geophys. Res. 100 (1995) 423–438.

[16] P.B. Kelemen, J.A. Whitehead, E. Aharonov, K.A. Jordahl, Experiments on flow focusing in soluble porous media with applications to melt extraction from the mantle, J. Geophys. Res. 100 (1995) 475–496.

[17] Y. Niu, Mantle melting and melt extraction processes beneath ocean ridges: Evidence from abyssal peridotites, J. Petrol. 38 (1997) 1047–1074.

[18] M.B. Baker, E.M. Stolper, Determining the composition of high-pressure mantle melts using diamond aggregates, Geochim. Cosmochim. Acta 58 (1994) 2811–2827.

[19] M.J. Walter, T.W. Sisson, D.C. Presnall, A mass proportion method for calculating melting reactions and application to melting of model upper mantle lherzolite, Earth Planet. Sci. Lett. 135 (1995) 77–90.

[20] R.J. Kinzler, Melting of mantle peridotite at pressures approaching the spinel to garnet transition: Application to mid-ocean ridge basalt petrogenesis, J. Geophys. Res. 102 (1997) 853–874.

[21] P.H. Nixon, Mantle Xenoliths, Wiley, New York, 1987.

[22] A. Nicolas, Structures of Ophiolite and Dynamics of Oceanic Lithosphere, Kluwer Academic, Dordrecht, 1989, p. 368.

[23] F. Boudier, E. Le Sueur, A. Nicolas, Structure of an atypical ophiolite: the Trinity Complex, eastern Klamath Mountains, California, Geol. Soc. Am. Bull. 101 (1989) 820–833.

[24] M. Cannat, D. Bideau, R. Hébert, Plastic deformation and magmatic impregnation in serpentinized ultramafic rocks

from the Garrett transform fault (East Pacific Rise), Earth Planet. Sci. Lett. 101 (1990) 216–232.
[25] R. Hébert, D. Bideau, R. Hékinian, Ultramafic and mafic rocks from the Garret Transform fault near 13°30′N on the East Pacific Rise: igneous petrology, Earth Planet. Sci. Lett. 65 (1983) 107–125.
[26] R. Hékinian, D. Bideau, M. Cannat, J. Franchteau, R. Hébert, Volcanic activity and crust–mantle exposure in the ultrafast Garret transform fault near 13°28′S in the Pacific, Earth Planet. Sci. Lett. 108 (1992) 259–273.
[27] R. Hékinian, D. Bideau, J. Franchteau, J.J. Cheminee, R. Armijo, P. Lonsdale, N. Blum, Petrology of the East Pacific Rise crust and upper mantle exposed in Hess Deep (eastern equatorial Pacific), J. Geophys. Res. 98 (1993) 8069–8094.
[28] Y. Niu, R. Hékinian, Basaltic liquids and harzburgitic residues in the Garrett transform: A case study at fast-spreading ridges, Earth Planet. Sci. Lett. 146 (1997) 243–258.
[29] T. Juteau, E. Berger, M. Cannat, Serpentinized, residual mantle peridotites from the MAR median valley, ODP Hole 670A (21°10′N, 45°02′W, Leg 109): Primary mineralogy and geothermometry, Proc. Ocean Drill. Progr. 106/109 (1990) 27–45.
[30] Y. Bassias, C. Triboulet, Petrology and P–T–t evolution of the Southwest Indian Ridge peridotites. A case study: east of the Melville Fracture zone at 62°E, Lithos 28 (1992) 1–19.
[31] J.E. Snow, H.J.B. Dick, Pervasive magnesium loss by marine weathering of peridotite, Geochim. Cosmochim. Acta 59 (1995) 4219–4235.
[32] S. Komor, D. Elthon, J. Casey, Serpentinization of cumulate ultramafic rocks from the North Arm Mountain massif of the Bay of Islands ophiolite, Geochim. Cosmochim. Acta 49 (1985) 2331–2338.
[33] H.J.B. Dick, Abyssal peridotites, very slow spreading ridges and ocean ridge magmatism, in: A.D. Saunders, M.J. Norry (Eds.), Magmatism in the Ocean Basins, Geol. Soc. London Spec. Publ. 42 (1989) 71–105.
[34] E. Bonatti, J. Honnorez, Sections of the Earth's crust in the equatorial Atlantic, J. Geophys. Res. 81 (1976) 4014–4116.
[35] M. Prinz, K. Keil, J.A. Green, A.M. Reid, E. Bonatti, J. Honnorez, Ultramafic and mafic dredge samples from the equatorial Mid-Atlantic Ridge and fracture zones, J. Geophys. Res. 81 (1976) 4087–4103.
[36] J.M. Sinton, Petrology of (alpine-type) peridotites from Site 395, DSDP Leg 45, Init. Rept. DSDP 45 (1978) 595–601.
[37] P.R. Hamlyn, E. Bonatti, Petrology of mantle derived ultramafics from the Owen Fracture zone, Northwest Indian Ocean: Implications for the nature of the oceanic upper mantle, Earth Planet. Sci. Lett. 48 (1980) 65–79.
[38] I.A. Nicholls, J. Ferguson, H. Jones, G.P. Marks, J.C. Mutter, Ultramafic blocks from the ocean floor Southwest of Australia, Earth Planet. Sci. Lett. 56 (1981) 362–374.
[39] E. Bonatti, G. Ottonello, P.R. Hamlyn, Peridotites from the Island of Zabargad (St. John), Red Sea: Petrology and geochemistry, J. Geophys. Res. 91 (1986) 599–631.
[40] R. Hébert, G. Serri, R. Hékinian, Mineral chemistry of ultramafic tectonites and ultramafic to gabbroic cumulates from the major oceanic basins and North Apennine ophiolites (Italy) — A comparison, Chem. Geol. 77 (1989) 183–207.
[41] R. Hébert, A.C. Adamson, S.C. Komor, Metamorphic petrology of ODP Leg 109, Hole 670A serpentinized peridotites: Serpentinization processes at a slow-spreading ridge environment, Proc. Ocean Drill. Prog. Sci. Results 106/109 (1990) 103–115.
[42] G.B. Piccardo, B. Messiga, R. Vannucci, The Zabargad peridotite — pyroxene association: Petrological constraints on its evolution, Tectonophysics 150 (1988) 135–162.
[43] T. Fujii, Petrology of peridotites from Hole 670A, Leg 109, Proc. Ocean Drill. Prog. Sci. Results 106/109 (1990) 19–25.
[44] M. Cannat, D. Bideau, H. Bougault, Serpentinized peridotites and gabbros in the Mid-Atlantic Ridge axial valley at 15°37′N and 16°52′N, Earth Planet. Sci. Lett. 109 (1992) 87–106.
[45] J. Girardeau, J. Francheteau, Plagioclase–wehrlites and peridotites on the East Pacific Rise (Hess Deep) and the Mid-Atlantic Ridge (DSDP Site 334): Evidence for magma percolation in the oceanic upper mantle, Earth Planet. Sci. Lett. 115 (1993) 137–149.
[46] S. Komor, T.L. Grove, R. Hébert, Abyssal peridotites from ODP Hole 670A (21°10′N, 45°02′W): Residues of mantle melting exposed by non-constructive axial divergence, Proc. Ocean Drill. Progr. 106/109 (1990) 85–101.
[47] S. Marshak, E. Bonatti, H. Brueckner, T. Paulsen, Fracture zone tectonics at Zabargad Island, Red Sea (Egypt), Tectonophysics 216 (1992) 379–385.
[48] Y. Niu, R. Batiza, DENSCAL: A program for calculating the densities of silicate melts and minerals as a function of temperature, pressure, and composition in magma generation environment, Comput. Geosci. 17 (1991) 679–687.
[49] Y. Niu, R. Batiza, In-situ densities of silicate melts and minerals as a function of temperature, pressure, and composition, J. Geol. 99 (1991) 767–775.
[50] D.R. Janecky, W.E. Seyfried, Hydrothermal serpentinization of peridotite within the oceanic crust: Experimental investigations of mineralogy and major element chemistry, Geochim. Cosmochim. Acta 50 (1986) 1357–1378.
[51] H.J.B. Dick, J.H. Natland, Late-stage melt evolution and transport in the shallow mantle beneath The East Pacific Rise, Proc. Ocean Drill. Prog. 147 (1996) 103–134.
[52] H.J.B. Dick, Partial melting in the Josephine Peridotite; I, The effect on mineral composition and its consequence for geobarometry and geothermometry, Am. J. Sci. 277 (1977) 801–832.
[53] M.J. O'Hara, Primary magma and the origin of basalts, Scott. J. Geol. 1 (1965) 19–40.
[54] D.H. Green, A.E. Ringwood, The genesis of basaltic magmas, Contrib. Mineral. Petrol. 15 (1967) 103–190.
[55] A.L. Jaques, D.H. Green, Anhydrous melting of peridotite at 0–15 kb pressure and the genesis of tholeiitic basalts, Contrib. Mineral. Petrol. 73 (1980) 287–310.
[56] E. Stolper, A phase diagram for mid-ocean ridge basalts: Preliminary results and implications for petrogenesis, Contrib. Mineral. Petrol. 74 (1980) 13–27.
[57] T.J. Falloon, D.H. Green, Anhydrous partial melting of

MORB pyrolite and other peridotite compositions at 10 kbar: Implications for the origin of MORB glasses, Mineral. Petrol. 37 (1987) 181–219.

[58] T.J. Falloon, D.H. Green, Anhydrous partial melting of peridotite from 8 to 35 kb and the petrogenesis of MORB, J. Petrol. Spec. Lithosphere Issue (1988) 379–414.

[59] M.J. O'Hara, The bearing of phase equilibria studies in synthetic and natural systems on the origin and evolution of basic and ultrabasic rocks, Earth Sci. Rev. 4 (1968) 69–133.

[60] Y. Bottinga, C.J. Allègre, Thermal effects of seafloor spreading and the nature of the oceanic crust, Tectonophysics 18 (1973) 1–17.

[61] Y. Niu, R. Hékinian, Spreading rate dependence of the extent of mantle melting beneath ocean ridges, Nature 385 (1997) 326–329.

[62] K. Hirose, I. Kushiro, Partial melting of dry peridotites at high pressures: Determination of compositions of melts segregated from peridotite using aggregates of diamonds, Earth Planet. Sci. Lett. 114 (1993) 477–489.

[63] S.R. Hart, A. Zindler, In search of bulk Earth composition, Chem. Geol. 57 (1986) 247–267.

[64] W.F. McDonough, S.-s. Sun, The composition of the Earth, Chem. Geol. 120 (1995) 223–253.

[65] E. Jagoutz, H. Palme, H. Blum, M. Cendales, G. Dreibus, B. Spettel, V. Lorenz, H. Wänke, The abundances of major, minor, and trace elements in the earth's mantle as derived from primitive ultramafic nodules, Proc. 10th Lunar Planet. Sci. Conf., 1979, pp. 2031–2051.